Packaging Technology and Science

WILEY

Packaging Technology and Science
An International Journal

RESEARCH ARTICLE OPEN ACCESS

Chemical Characterization of Postindustrial Recycled Polyethylene Terephthalate Obtained From Multilayer PET/PE Sheets: A Baseline Study on Safety Aspects

Isabela F. A. Daras[1] | Srishti Singh[1] | Tiago Vieira[1] | Joel Pereira[2] | Patrícia Guerreiro[2] | Clara Sousa[1] | Fátima Poças[1,2]

[1]Universidade Católica Portuguesa, CBQF Centro de Biotecnologia e Química Fina-Laboratório Associado, Escola Superior de Biotecnologia, Porto, Portugal | [2]CINATE, Escola Superior de Biotecnologia, Universidade Católica Portuguesa, Porto, Portugal

Correspondence: Fátima Poças (fpocas@ucp.pt)

Received: 21 July 2025 | **Revised:** 6 October 2025 | **Accepted:** 22 October 2025

Funding: This work was supported by the National Funds from FCT - Fundação para a Ciência e a Tecnologia (UIDB/50016/2020).

Keywords: multilayer trays | oligomers from PET | PE layer separation | PET degradation compounds | tie-layer adhesive removal

ABSTRACT

Trays made from thermoformed plastic sheets represent the second major application of PET packaging after beverage bottles. PET recycling is promoted in the European Union, where ambitious targets for recycling rates and recycled content in packaging have already been established. However, PET trays, contrary to most beverage bottles, pose recycling challenges due to multilayer structures with polyethylene (PE) tie-layers and barrier materials. In this study, a delamination process using a hot alkaline solution was applied to postindustrial multilayer PET/PE thermoforming waste to recover PET flakes and produce sheets containing varying rPET contents. The process showed >95% PE removal. Sheets incorporating rPET exhibited increased yellowness, haze and decreased intrinsic viscosity but maintained suitable thermal properties for thermoforming applications. Among thermal properties, only the cold crystallization temperature was notably affected. Results from FTIR and GC–MS analyses, combined with principal component analysis, were used to differentiate the samples containing rPET and confirmed chemical similarity between recycled and virgin PET, although residual tie-layer compounds and delamination process residues were detected. Overall migration tests yielded values below regulatory limits, while untargeted GC–MS screening revealed the presence of degradation products, surfactant residues and oligomers. As expected, sheet production led to a decrease in the concentration of volatile and semivolatile migrants. However, higher concentrations of oligomers, particularly 1st series cyclic trimers, were quantified by LC–MS in the sheets compared to the flakes, indicating thermal stress effects during extrusion. Several PET degradation compounds were also identified in the sheets, highlighting the need for further migration studies to assess safety. These findings demonstrate that alkaline delamination is an effective strategy for recovering PET from multilayer tray waste although safety assessment of oligomers and specific migrants remains essential for food-contact applications.

1 | Introduction

Polyethylene terephthalate (PET) has a market in Europe estimated at 5 million tonnes, of which 97% was for packaging purposes [1–3]. A major amount of PET packaging is used in the production of beverage bottles, while the second main application was in the production of sheets for tray thermoforming. Trays are typically wide and flat rigid packaging with varying

depths. Similar to bottles, trays are also used for primary packaging of foods but mainly for solid food products, such as fresh meat, cheese, nuts, fruits, vegetables and baked goods.

As other nonbiodegradable polymers, PET has undesirable effects on the environment if its waste is not handled properly. Material circularity through recycling is considered a viable solution for preventing such impacts [4, 5] and promoted by the PPWR Packaging and Packaging Waste Regulation (EU) 2025/40.

PET articles following the principles of design-for-recycling can be recycled multiple times especially after decontamination processes where the degradation effects of reprocessing are reversed [6]. This is true for PET bottles, wherein bottle-to-bottle recycling has already been established [7]. However, other PET articles such as trays are still being developed to improve their circularity, as the current situation for most rPET tray production is through a bottle-to-tray scheme [8]. Compared to PET bottles, trays are harder to recycle due to various factors such as the presence of a higher level of contamination (food residues, labels, adhesives, colours, etc.), insufficient collection and sorting volume as well as lower yield and recycled plastic quality [3]. PET bottles and trays are usually collected together, but PET multilayer trays are considered contaminants on PET bales and further sorted. The difference in the intrinsic viscosities (IVs) of PET trays compared to PET bottles results in lower recycled material quality [9]. Higher IV is required for the production of PET beverage bottles, especially for carbonated drinks, around 0.78–0.85 dL g^{-1}, while the minimum IV of PET sheets [10] is only 0.70 dL g^{-1}. In cases where the two materials are recycled together, trays are mixed in low quantities to minimize the effect on the IV of final products. PET tray wastes are sometimes converted into low-quality food-grade rPET with limited application, or used in the fibre and textile industry, incinerated for energy recovery, or disposed of in landfills [11, 12].

Another challenge in PET trays recycling is their composition. Most trays (ca. 60%) are composed of multiple layers of different materials, including polyethylene (PE) for better heat sealing (Figure 1) and/or ethylene vinyl alcohol (EVOH) for high barrier. These multilayer structures often do not meet the criteria set for conventional mechanical recycling [13–15].

Compatibility with recycling processes is related to the quality of the resulting recycled material. For mechanical recycling, which is the most common process, recycling mixed polymers, particularly immiscible polymers, results in poor mechanical properties [16]. The varying proportions of polymer components in tray wastes may lead to inconsistent quality of the recycled material, as the trays have different compositions. Although compatibilisers can be added to improve the miscibility of polymer blends, the heterogeneity of the polymer wastes makes the whole process complex due to adjustments in the type and quantity of compatibiliser that should be applied [17]. Hence, in such cases, component separation is necessary prior to recycling individual components [12].

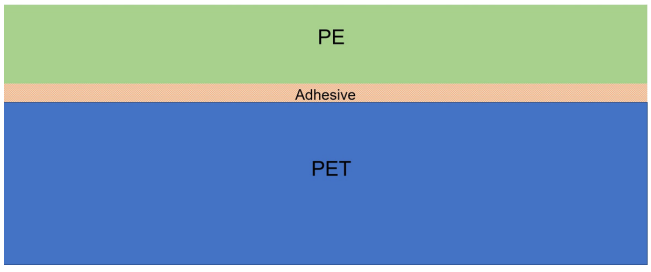

FIGURE 1 | Depiction of the cross-section of the ground PIW (PET/PE flakes).

In addition to compatibilisation with additives, several techniques have been proposed for recycling multilayer packaging including delamination, depolymerisation and selective dissolution-precipitation [18, 19]. For PET-based trays, techniques have also been developed based on the above-mentioned technologies to address the problems associated with recycling multilayer materials. Table 1 shows some of the recently developed methods and techniques that were either specifically designed for or tested on PET-based multilayer trays or on mixed wastes containing PET-based multilayer trays. The processes focused on the separation and recovery of individual polymer components especially PET. It should be noted that most techniques developed to recycle PET-based multilayer trays employ chemical recycling by depolymerisation, which can yield higher quality recycled material, even from waste that is considered difficult to recycle, such as postconsumer multilayer trays [15, 20]. However, the major disadvantage of this technology is that it is energy-intensive [21].

In the trays thermoforming process, large amounts of waste in the form of the sheet skeleton corresponding to 15%–50% of the original sheet, are created. Rejected scraps are also considered as postindustrial waste (PIW). Because these wastes have not yet been used for packaging, they are considered clean and are typically reground and re-extruded with virgin materials into new sheets [22]. However, this cannot be performed directly if the sheet has a multilayer structure. Delamination prior to regrinding and re-extrusion is considered a promising technique, cost-effective and easier to perform than other techniques, such as chemical recycling by depolymerisation because it does not require a specific infrastructure and usually utilizes a single solvent for its operation [23]. However, because the resulting recycled materials are heavily influenced by feedstock quality, this technique should be used for homogenous feedstock.

One of the methods of delamination is through the use of hot alkaline solutions, typically used as washing agents to hydrolyse bonds in acrylate or acetate-based adhesives and remove contaminants such as glues from labels, dirt, inks, oils as well as volatile organic components [24–26]. This washing step can potentially be used for delamination of PET-based trays and layer separation for recovery of the PET fraction. The process can be applied to PIW, as well as postconsumer waste of PET-based multilayer trays. However, limited studies have been conducted on the recommended approach especially regarding the effects on the quality and safety of the recycled materials produced.

This study aims to evaluate the safety and quality of the rPET obtained from postindustrial multilayer PET/PE waste and the resulting sheets, as well as to assess the performance of the recycling process. The objective is to obtain a chemical

TABLE 1 | Recently developed recycling methods applied to multilayer PET-based trays.

Developer	Method	Description	Reference(s)
GAIKER Technology Centre and University of the Basque Country	Bio-solvolysis reaction	Catalytic glycolysis using biobased monoethylene glycol (BioMEG) as a depolymerisation agent to yield bis(2-hydroxyethyl) terephthalate (BHET) monomer. Optimal conditions: PET/BioMEG molar ration = 1:7.6, 1% (m/m) zinc acetate catalyst, 185°C and 250 rpm stirring rate. Activated carbon was used to purify further the monomer by removing the colour and decreasing the metal content.	Amundarain et al., 202
REPETCO Innovations S.L.	Separation through application of superheated steam vapour to induce heat and mechanical shocks.	Ground multilayer plastics are put into a container, which is then pressurized using overheated vapour until the pressure reaches 1–12 bar and the temperature of 100°C–191.12°C. The ground material is then transferred to a discharge tank at a relative pressure between −0.7 and 0.1 bar and a temperature between 15°C and 25°C. Then transferred again to a mechanical separation unit. The heat and mechanical shocks that was produced from the process promotes the weakening and breaking of the chemical bonds between the layers without using any other chemical products.	Escudero et al., 2024
Carbios	Bio-recycling through enzymatic PET hydrolysis	The use of enzyme LCC^{ICCG} to hydrolyse PET into its monomers: ethylene glycol (EG) and terephthalic acid (TPA). With 98% conversion achieved in 24 h, which is better than other isolated PET hydrolases.	Arnal et al., 2023
Garbo	ChemPET	Chemical recycling through innovative glycolysis of PET to yield BHET. The process aims to produce chemically recycled PET, which is comparable with virgin sources.	Garbo, 2023
RITTEC Umwelttechnik GmbH and partners	revolPET—selective depolymerisation	Selective depolymerisation of PET to EG and TPA by alkaline hydrolysis in a twin-screw extruder. The process yield is up to 95% and other polymer components were deemed unchanged and can be separated by filtration.	Franco et al., 2023, Biermann et al., 2021

(Continues)

TABLE 1 | (Continued)

Developer	Method	Description	Reference(s)
Ghent University	Alkaline hydrolysis	Two-step alkaline hydrolysis under mild conditions to yield PET monomers (TPA and EG). At optimal conditions: 60:40 (v/v) EtOH:H_2O, 5% (m/m) NaOH, 80°C, about 95% PET conversion was achieved after 20 m. Other polymers were deemed unchanged and were separated by filtration.	Ügdüler et al., 2020
Sulayr Global Service SL	Delamination	Separation of individual components of trays (PET/EVOH/PE) laminated using polyurethane-based adhesives through the use of alkaline bleaches as separating agent	García Fernández, 2013
Wageningen University	Enzymatic depolymerization	Polyester hydrolases from *Pichia pastoris* yeast were used to depolymerize PET from PET/PE trays. High yields were obtained using unpurified enzyme and high PET-PE loading at 10%–20% (w/w) PET-PE achieving ≥94% PET depolymerization and ≥80% terephthalic acid (TPA) recovery. A scale-up process using 4.5 kg of PET-PE achieved ≥95% PET depolymerization. TPA was successfully repolymerized into PET.	van Vliet et al., 2025

characterization of the recycled PET (rPET) with relevance for safety aspects, as a baseline study for future postconsumer waste recycling studies.

2 | Materials and Methods

2.1 | Recovery of PE Terephthalate From PIW and Production of Sheets

Multilayer PIW from the thermoforming process (trimmings from sheets composed of PET laminated with PE using acrylic-based adhesives) was supplied by Evertis Iberica S.A. (Portalegre, Portugal). PIW was ground into flakes with an average size of 10 mm and loaded into a batch reactor. Delamination of flakes by selective dissolution of the tie-layer using an alkaline solution was performed. An alkaline solution (NaOH 10% w/w) was used to facilitate the dissolution of the adhesives. A nonionic surfactant (1% w/w) together with an antifoam solution was added to improve the surface tension between the solution and the flakes. The solution/solid ratio (w/w) was greater than 2. The reactor was heated to 75°C and stirred continuously for 24 h. The first separation was done by differences in density in which the settled PET materials were collected to undergo warm rinsing and drying using hot air. The second separation was done through air elutriation to remove any trapped PE and other fine materials from the dried PET. All recovered PET materials, now referred to as rPET, were stored in bags until further processing.

PET sheets with three (3) contents of rPET were produced (Table 2). The PET sheet made from only virgin PET materials (S-Vg) served as the control. Antiblocking masterbatch (fatty acid amides) was added to reduce blocking of the sheets in the roll. The sheets were produced through industrial cast film extrusion using a single-screw extruder (SML Maschinengesellschaft mbH, Redlham, Austria) operating at a temperature of 80°C–280°C at different zones with a screw speed of 37 rpm. The final thickness of all PET sheets was 300 μm.

2.2 | Analysis and Characterization of the Samples

The PET flakes and sheets were subjected to various physico-chemical analyses (Table 3).

2.2.1 | Residual PE

The amount of residual PE in the rPET flakes was measured according to EN 15348:2024 Annex C. Briefly, 200 g of sample flakes was evenly spread in an aluminium tray and placed inside a muffle furnace preheated at 200°C for 1 h, after

TABLE 2 | Composition of samples.

Sample code	Identity	Percentage (%, m/m) composition		Thickness (μm)
		rPET	vPET	
F-Ml	PET/PE flakes	—	—	—
F-Rc	rPET flakes	—	—	—
S-Rc	PET sheets	100	0	300
S-Mx	PET sheets	20	80	300
S-Vg	PET sheets	0	100	300

Abbreviations: F, flakes; Ml, multilayer; Mx, mix; Rc, recycled; S, sheets; Vg, virgin.

TABLE 3 | Analyses and tests conducted.

Analysis	Flakes		Sheets		
	F-Ml	F-Rc	S-Rc	S-Mx	S-Vg
Residual PE		✓			
Optical properties			✓	✓	✓
Moisture content		✓			
Intrinsic viscosity		✓	✓	✓	✓
Thermal properties	✓	✓	✓	✓	✓
Fourier transform infrared (FTIR) spectroscopy			✓	✓	✓
Overall migration			✓	✓	✓
Potential migrants through untargeted screening	✓	✓	✓	✓	✓
PET cyclic dimer and trimer		✓	✓	✓	✓

Abbreviations: F, flakes; Ml, multilayer; Mx, mix; Rc, recycled; S, sheets; Vg, virgin.

which the flakes were cooled down and inspected thoroughly. Discoloured materials corresponding to polyolefin (PE) impurities were separated and weighed. Results were expressed in mg kg^{-1}.

2.2.2 | Optical Properties

Colour of the PET sheet samples was measured based on the CIELab method (Spectrophotometer CM-5) and the results were processed in SpectraMagic NX software (Konica Minolta, Tokyo, Japan). Haze was also measured using the same instrument. Calibration using the built-in zero (0%) and white (100%) calibration plates was performed prior to the testing of the samples. Spectrophotometric analysis of the sheet samples was measured using transmittance mode.

2.2.3 | Moisture Content

The moisture content of the rPET flakes was measured gravimetrically using an MS-70 moisture analyser (A&D Precision Inc., California, USA).

2.2.4 | Intrinsic Viscosity

The IV of the rPET flakes and PET sheets was determined according to ISO 1628-5 (Lovis 2000 ME Microviscometer Anton Paar GmbH, Graz, Austria). A sample solution with a concentration of 0.001 g mL^{-1} was prepared by dissolving 0.30–0.35 g of mono-material PET sample in a vial with 30 mL of dichloroacetic acid (Sigma-Aldrich, Missouri, USA) following stirring at 75°C for 50 min until full dissolution. The mixture was then cooled down in a water bath prior to injection. Measurements were taken at 25°C. An average value of 6 measurements was taken and the IV was calculated using the Billmeyer relationship [27].

2.2.5 | Thermal Properties

Thermal transitions of materials were measured through differential scanning calorimetry (DSC) technique following ASTM D 3418 (DSC 204 F1 Phoenix, NETZSCH, Bayern, Germany). It determined the temperatures of melting (T_m), cold crystallization (T_{cc}) and glass transition (T_g), as well as the percentage (%) crystallinity (Figure S4). The tests were performed in triplicates for both flakes and sheet samples. Two (2) ± 0.5 mg of sample were weighed into a DSC aluminium crucible. The test ran with two heating cycles at a heating rate of 10°C per min, under nitrogen flux of 40 mL per min and temperature range from 25°C to 300°C. The results were analyzed in Proteus software v7 (NETZSCH, Bayern, Germany). The percentage (%) crystallinity was computed using the following equation [28]:

$$\%\,Crystallinity = \left[(\Delta Hm - \Delta Hc) / \Delta Hm^{\circ}\right] \times 100 \quad (1)$$

ΔHm is the heat of melting equivalent to the area under the peak of T_m, expressed as J g^{-1}, ΔHc is the heat of cold crystallization equivalent to the area under the peak of T_{cc}, expressed as J g^{-1}, and $\Delta Hm°$ is the heat of melting of 100% crystalline PET equivalent to 140 J g^{-1}.

2.2.6 | Fourier Transform Infrared spectroscopy

The mid-infrared spectra of the PET sheet samples were obtained within the wavenumber interval of 4000–600 cm^{-1}, with a resolution of 4 cm^{-1} with a deuterated triglycine sulphate (DTGS) detector (PerkinElmer Spectrum BX FTIR System spectrophotometer, Massachusetts, USA). Spectra were

acquired in diffuse reflectance mode through a Gladi attenuated total reflectance (ATR) accessory (PIKE Technologies, Wisconsin, USA). Each spectrum resulted from 32 scan co-additions. Films were placed in the ATR crystal and a constant pressure was applied. The ATR crystal was cleaned and a background was acquired between each sample. Five spectra per sample were acquired.

The spectra were modelled through a principal component analysis (PCA) [29]. Prior modelling, spectra were preprocessed with standard normal variate (SNV) [30] and the Savitzky–Golay filter (15 smoothing points, 2nd-order polynomial and 2nd derivative) [31] and further mean-centred. Spectral preprocessing and modelling were performed in MATLAB R2023a (MathWorks, Natick, Massachusetts, USA) and PLS Toolbox 9.2.1 (Eigenvector Research, Manson, Washington, USA).

2.2.7 | Overall Migration

The overall migration of the PET sheet samples was measured according to EN 1186-3:2022 through total immersion in a conventional oven using the following three aqueous simulants: 3% (m/v) acetic acid (WVR, Pennsylvania, USA), 10% and 50% (v/v) ethanol (Fisher Chemical, Pennsylvania, USA). Sheets were cut into 1-dm^2 samples, immersed in 100 mL of aqueous simulant and placed in an oven maintained at 40°C for 10 days. Simulants were then evaporated and the weight of the residue was noted. The results were calculated using the formula and expressed as milligrams of residue per dm^2 (mg dm^{-2}) of the surface area of the sample [32]:

$$M = \left(m_a - m_b\right) / S \tag{2}$$

M is the overall migration into the food simulant (mg dm^{-2}), m_a is the mass of the residue from the test specimen after evaporation of the food simulant, m_b is the mass of the residue from the blank of the food simulant, and S is the surface area of the test specimen exposed to the food simulant.

2.2.8 | Potential Migrants Through Untargeted Screening by GC–MS

Untargeted gas chromatography coupled with mass spectrometry (GC–MS) analysis was done to detect identify and semiquantify both intentionally and nonintentionally added substances (respectively, IAS and NIAS) with the potential to migrate. Samples were prepared and tested following the Petcore Europe guidelines [33]. Gas chromatography coupled with mass spectrometry (GC–MS) was performed using two different extraction techniques: headspace extraction to analyze volatile compounds and liquid extraction for semivolatile compounds. A GC–MS system was used (Scion 456-GC, Bruker, Massachusetts, USA) with a separation column 30 m × 0.25 mm × 0.25-μm Zebron ZB-5MS plus (Phenomenex, California, USA). The carrier gas was helium (1 mL per min).

2.2.8.1 | Sample Preparation (Headspace and Liquid Extraction). All flakes and sheet samples were cryogenically ground with a 0.75 mm sieve (ZM 200 Ultra Centrifugal Mill [Retsch GmbH, Haan, Germany]) and kept in headspace vials. One (1) ± 0.005 g of ground samples was placed in 20-mL headspace vials. Duplicate analysis was performed and one blank was prepared.

For the headspace extraction, 1 μL of an internal standard (IS) solution of deuterated dodecane (Sigma-Aldrich, Missouri, USA) in methanol (0.03 mg mL^{-1}, m/v) was added to two vials, while the other vial was a blank. The samples were then subjected to thermal desorption at 200°C for 1 h using a Combi PAL autosampler (CTC Analytics AG, Zwingen, Switzerland) prior to GC analysis. The injection volume was 1 mL (split 1:10) at 250°C. The oven temperature programme was set to 40°C per 5 min, raised to 10°C per min until 320°C. The MS ionization mode was electron ionization (EI) at 70 eV. Full scan was made between 33 and 350 m/z.

For the liquid extraction, 10 mL of dichloromethane (Fisher Chemical, Pennsylvania, USA) was added to each vial. The vials were incubated at 40°C for 3 days. Samples were then filtered and washed twice with 5-mL dichloromethane, following evaporation to dryness under nitrogen and reconstitution with 1-mL IS solution of deuterated dodecane in methyl *tert*-butyl ether (MTBE) (Sigma-Aldrich, Missouri, USA). The solution was then filtered in a 0.45-μm polytetrafluoroethylene (PTFE) filter and transferred to vials for GC–MS analysis. The injection volume was 1 μL (splitless for 0.75 min) at 280°C. The oven temperature programme was set to 50°C for 3 min, raised to 10°C per min until 320°C for 15 min. The MS ionization mode was EI at 70 eV. A full scan was made between 33 and 700 m/z.

2.2.8.2 | Tentative Identification of Peaks. All resulting chromatograms were analyzed in MS Data Review software v8.2.1 (Bruker, Massachusetts, USA). Tentative identification of compounds was performed by comparing mass spectra of each peak to the NIST Mass Spectral Library v2.3 (2017). Judgement was done by considering the match factor, reverse match factor and probability of the match. Additionally, the Kovats retention index (RI) was calculated to compare with library values.

2.2.8.3 | Semiquantification of Compounds. A mixture of standards was used for the semiquantification of compounds (see Table S1 in Supplementary Information). The substances were assigned a response factor (RF) corresponding to the component representing the class in the mixture of standards. Otherwise, the substance was semiquantified based on the RF of deuterated dodecane. The results were expressed as μg g^{-1}. Estimated migration values were calculated assuming total transfer and using a medium-sized PET tray with a capacity of 0.5 L, weighing 11 g as reference. The semiquantitative results were subjected to PCA (IBM SPSS Statistics 26 for Windows, IBM Corp., Armonk, NY, USA).

2.2.8.4 | Toxicity Assessment of the Determined Potential Migrants. Each tentatively identified compound in the GC–MS analysis was classified according to the Cramer Class [34] using Toxtree v3.1.0 (Ideaconsult Ltd., Sofia, Bulgaria).

2.2.9 | Quantification of PET Cyclic Dimer and Trimer by Target LC–MS

PET 1st series cyclic dimer and trimer were determined by targeted liquid chromatography coupled to triple-quadrupole mass spectrometry (LC–QQQ–MS) after total dissolution of the polymer. Triplicate aliquots of the sample (0.400 ± 0.005 g) were dissolved in 4 mL of 1,1,1,3,3,3-hexafluoro-2-propanol (HFIP) at 40°C for 24 h. After complete dissolution, 8-mL LC-grade methanol was added dropwise with gentle mixing and the solution was kept at 4°C for 1 h. Samples were centrifuged (2500 rpm, 15 min); the supernatant was decanted, washed once with 2-mL methanol, filtered through a 0.2-μm PTFE syringe filter and transferred to 2-mL LC vials for analysis.

Chromatographic separation was performed on a reversed-phase C18 analytical column (100 × 2.1 mm, 3 μm) coupled to a 50 × 2.1 mm delay column, maintained at 40°C. Mobile phase A was 5 mM ammonium acetate in water and mobile phase B was 5 mM ammonium acetate in methanol. The flow rate was 0.40 mL min^{-1} with a gradient of 5% B (0 min) to 95% B at 10.0 min, held to 13.0 min. The injection volume was 5 μL.

Mass spectrometry was carried out on a Bruker EVOQ Elite triple quadrupole with electrospray ionization in positive mode (ESI+), operated in multiple reaction monitoring (MRM). The predominant molecular ions were the ammonium adducts $[M + NH_4]^+$. The monitored transitions were: cyclic dimer, m/z 371.1 → 149.0 (quantifier) and 371.1 → 193.1 (qualifier); cyclic trimer, m/z 529.2 → 149.0 (quantifier) and 529.2 → 193.1 (qualifier). Detailed MS source and acquisition parameters (e.g., source temperature, gas flows, voltages, collision energies and dwell times) are provided in Supplementary Information Table S2.

Calibration was performed using standards of ethylene terephthalate cyclic dimer ($[TPA\text{-}EG]_2$, CAS No. 24388-68-9) and trimer ($[TPA\text{-}EG]_3$, CAS No. 7441-32-9) (Toronto Research Chemicals, Canada), with calibration and performance data summarized in Supplementary Information Table S3. Five-point calibration curves (HFIP stock diluted in methanol) showed linearity with $R^2 > 0.99$. Method performance was further evaluated by determination of limit of detection (LOD, S/N ≈ 3) and limit of quantification (LOQ, S/N ≈ 10). Final concentrations were expressed as μg g^{-1} of PET (mean ± SD, $n = 3$).

2.3 | Statistical Analysis

Comparison of group means was done through the application of one-way analysis of variance (ANOVA) in OriginPro 2024b v10.1.5.132 (OriginLab Corp., Massachusetts, USA). A significance level of $\alpha = 0.05$ was used and differences between means were considered statistically significant when $p \leq \alpha$. Tukey's test was used to assess the significance of differences between pairs of group means.

3 | Results and Discussion

3.1 | Recovery of PET Flakes

The ground multilayer PIW consisting of the skeleton resulting from trays thermoforming was delaminated to recover PET flakes and the samples were coded as F-Ml and F-Rc, respectively. Almost 85% of the weight of the multilayer sheet is composed of PET and the remaining 15% is the PE layer. The residual PE content measured in the rPET flakes is 1000 mg kg^{-1}, which is equivalent to more than 95% removal of the PE from the flakes. The residual content of PE in the rPET flakes is difficult to determine more precisely using the furnace test, because some of the residual PE sticks to the rPET flakes during the test. As a consequence, a fraction of the PE mass weighed is a combination of PE and PET. Therefore, the delamination efficiency is expected to be higher than 95%.

After the delamination process, the recovered rPET has a moisture content of 1.07% and an IV value of 0.68 dL g^{-1}.

3.2 | Optical Properties of the Sheets

Spectrophotometric analysis of the sheets showed slight differences in terms of colour and haze (Table 4). Higher values for parameter b^* (yellowness-blueness), indicating yellowing of the material, and slightly for a^* (redness-greenness), were obtained for the sheet S-Rc compared to standard S-Vg. A lower value for L^* (lightness) was obtained, indicating darkening. No significant difference was observed in all colour parameters between S-Vg and S-Mx. These differences in colour parameters resulted in a higher ΔE value for S-Rc. A correlation between the amount of rPET and the L^*, b^* and ΔE values has already been reported [35] as well as an inverse relationship between rPET content and L* value. The ΔE value increases with increasing rPET content. Nevertheless, both sheets containing rPET comply with the Petcore Europe standard [36].

Changes in the optical properties of PET are due to various factors. Yellowing is mainly due to the degradation of PET that leads to the formation and accumulation of light-absorbing chromophores. Examples of this include hydroquinone, quinone moieties, β-scission of the ester moieties, stilbenes and biphenyls. The strong and broad-band optical absorption of these chromophores in the ultraviolet and visible spectral regions

TABLE 4 | Optical properties of the PET sheet samples.

Parameters	S-Rc	S-Mx	S-Vg
L^*	95.98 ± 0.01[b]	96.08 ± 0.02[a]	96.05 ± 0.02[a]
a^*	0.16 ± 0.01[a]	0.14 ± 0.01[b]	0.14 ± 0[b]
b^*	0.54 ± 0.03[a]	0.39 ± 0.02[b]	0.40 ± 0.03[b]
ΔE	0.16	0.03	—
% Haze	1.06 ± 0.20[a]	0.78 ± 0.52[a]	0.42 ± 0.06[a]

*Values associated with the same letter horizontally are statistically equivalent ($\alpha = 0.05$).

gives a yellowish appearance [35]. However, yellowing can also be due to the incomplete dissolution of the polyacrylate tie-layer followed by thermal degradation.

In terms of haze, higher values were obtained by S-Rc and S-Mx indicating less transparency when compared to the standard sample S-Vg. The typical % haze of PET used in the industry is 0.5%[1]. However, tolerance up to 7% haze is the standard practice in sheet extrusion [36]. A good linear correlation between haze and rPET content was also reported in the literature [35].

Haze formation could be due to thermally induced crystallization. The transparent appearance of PET is due to the alignment of very small crystals formed by mechanically induced crystallization. However, when PET is heated to temperatures above the glass transition temperature (T_g), thermally induced crystallization occurs. In this case, randomly oriented lamellar structures that grew outward spherically from a nucleation site cause a hazy appearance in those regions of the PET [37, 38]. The increase in haze can also be due to residual PE, because as this and PET are immiscible polymers, combining them would result in light scattering due to the difference in the refractive indices of the two phases [39].

3.3 | Intrinsic Viscosity

Intrinsic viscosity (IV) of PET is a key rheological parameter that affects processing and mechanical properties of the final product and its application and performance. IV is linearly related to the polymer's average molecular weight [40]. The IV for PET thermoforming sheet applications usually ranges [10] from 0.70 to 1.00 dL g^{-1}.

The results show significantly different IV values for the samples. Lower IV values were observed with increasing rPET content. Sample S-Vg obtained a value within the industrial standard range at 0.72 ± 0.0035 dL g^{-1}. The samples S-Rc and S-Mx had lower values, 0.64 ± 0.0029 and 0.68 ± 0.0006 dL g^{-1}, respectively. An inverse relation between rPET content and IV value was reported [41] consistent with the obtained results. Thermal and hydrolytic degradation in mechanical recycling greatly affects the chemical composition and structure of PET, which in turn affects its IV [42].

3.4 | Thermal Properties

Thermal properties are important for defining the processing conditions [43–45]. For instance, thermoforming temperatures of PET are typically set to 125°C–165°C, which is above the T_g to avoid the brittle state of PET, while T_m determines the extrusion temperature. Results are detailed in Supplementary Information (Table S5).

The process of recovery and separation of the PET layer did not affect the thermal properties of the flakes as no significant difference was observed for T_m and T_g of the flakes. However, the sample F-Rc did not exhibit the pronounced peak for cold crystallization.

For the sheet samples, the results for T_m and T_g are consistent with values reported in the literature [43] and also no statistically significant differences were noted for the samples with rPET compared to S-Vg. The melting temperature of PET was recorded around 250°C and T_g around 79°C. However, significantly lower values were observed for T_{cc} of S-Rc compared to S-Vg. It was reported that rPET crystallizes more readily than vPET due to shorter chains that act as nuclei for crystallization. The % crystallinity of the samples also varied and was relatively lower suggesting a more amorphous state for the sample S-Vg. These observations are important to note because this can affect the elongation at the point of breaking during the thermoforming process [46].

3.5 | IR Spectroscopy

Infrared (IR) spectra of PET sheet samples were presented in Figure 2A. Spectra presented a very similar pattern among samples, which was quite expected, exhibiting typical PET infrared absorption bands [47], namely, a sharp band at 1710 cm^{-1} due

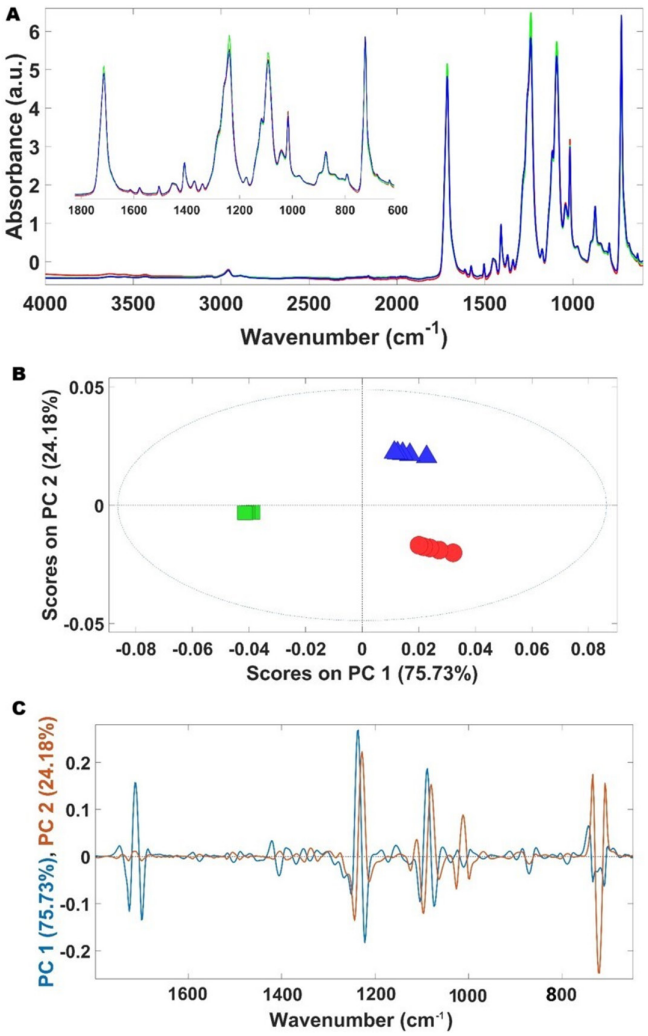

FIGURE 2 | (A) Mean infrared spectra of the PET sheets. Legend: S-Rc (—); S-Mx (—); and S-Vg (—). (B) Scores map of the PCA model developed with the infrared spectra in the region 1800–650^{-1}. (C) Loadings plot of the PCA model. Legend: S-Rc (■); S-Mx (▲); S-Vg (●).

to the C=O stretching; at 1408 cm^{-1} due to the stretching of the aromatic ring; at 1370 and 1340 cm^{-1} due to the CH_2 wagging of glycol; two broad bands at 1230 and 1090 cm^{-1} due to ester C=O stretching; at 1017 cm^{-1} from the benzene vibration (in plane); at 970 and 845 cm^{-1} due to C–O stretching and CH_2 rocking of glycol, respectively; and at 870 and 723 cm^{-1} due to out of the plane benzene vibrations.

Few differences were noted among IR spectra of the analyzed PET sheet samples with sample S-Rc being the most different. Sample S-Rc appeared to have slightly intense bands at 1710 cm^{-1}; at 1230 and at 1090 cm^{-1} being all related to C=O vibrations. These absorbances are probably due to residual (nonremoved) polyacrylate tie-layer, and therefore, it may be concluded that the alkaline washing process does remove the majority of the tie-layer, but not all.

A high infrared spectral similarity could be expected between the recycled and not recycled samples indicating that chemical composition is similar. However, it was necessary to clarify if those small spectral differences could be attributed to specific chemical compounds formed in the recycling process or if they were just random contaminants. Therefore, a PCA was performed to evaluate possible clusterisation among the PET sheet samples' IR spectra.

The first two principal components (PC1 + PC2) encompassed 99.9% of the spectral variability. Analyzing the PCA scores map together with the corresponding loadings plot, it is observed that samples are separated in clusters, corroborating the samples' composition (Figure 2B). The S-Rc samples are separated from (S-Vg + S-Mx) samples in PC1 with over 75% of spectral variability meaning that those samples are the most dissimilar ones. On the other hand, S-Vg and S-Mx samples are closer in the PCA scores map because they are more similar samples (it should be noted that S-Mx samples possess 80% of vPET and only 20% of rPET). In this context, the PCA corroborates the composition of the samples but also rules out the possibility that the observed small spectral differences are due to random contaminations.

Additionally, the PCA loadings plot was used as a tool to clarify the differences in the sample's chemical composition. The corresponding PCA model loadings (Figure 2C) allowed us to infer about the bands that mainly impacted the observed PET samples discrimination. Specifically, PC1 higher loadings were observed between 1732–1702 cm^{-1} due to C=O stretching of esters, aldehydes and ketones; 1242–1222 cm^{-1} due to esters C=O stretching; and 1112–1072 cm^{-1} due to C–O–C and/or C–OH stretching from ethers and/or alcohols. Sample S-Rc was discriminated between S-Vg and S-Mx in PC1 meaning that the above-mentioned classes of compounds were differently present in both types of samples (recycled/virgin). Regarding the discrimination between samples S-Vg and S-Mx, which occurred in PC2, the higher loadings were noticed between 1242 and 1222 cm^{-1}; 1102 and 1082 cm^{-1}; 1028 and 1010 and 738–712 cm^{-1}. These wavenumbers are linked to vibrations of C=O from esters, C–O–C and/or C–OH stretching from ethers and/or alcohols, in-plane and out-of-plane benzene vibrations and of mono or meta aromatic substituted rings [47–49]. These findings suggest that the chemical composition of these two sheets samples just slightly varied since most of the spectral differences were denoted in typical PET infrared vibration bands. As a conclusion the FTIR allows us to discriminate between samples in spite of the small differences between the spectra and therefore can be a relevant tool for monitoring incorporation of recycled material.

3.6 | Overall Migration, Untargeted Screening, Oligomers and Safety Evaluation

Overall migration values obtained for sheets were less than the limit of quantification (LOQ)—2.0 mg dm^{-2}, for all samples and all simulants. This result is not uncommon for PET-based materials where typical low overall migration values are observed.

3.6.1 | Untargeted Screening by GC–MS

This section presents the results obtained by GC–MS to screen and identify substances present in the sample materials (both flakes and sheets) that can potentially migrate. Examples of chromatograms obtained by headspace and by liquid extraction analyses are reported in Supplementary Information (Figures S1 and S2). A list of the 20 most abundant substances tentatively identified by GC–MS is presented in Table S4 (Supplementary Information). The information includes the identification of the compounds, the chemical group, the Cramer Class of toxicity, the concentration in the material and the migration estimated by calculation (Section 2.2.8.3). The chemical groups tentatively identified and the result of their semiquantification are presented in Figure 3A.

The flakes before processing (Sample F-Ml) yielded 147 peaks, mostly aldehydes and ketones. Butanal and pentanal are the most abundant substances detected in the sample. Tris(2,4-di-*tert*-butylphenyl) phosphate, which is the oxidized version of the stabilizer Irgafos 168, was also present in high concentration. As compared to other samples, a higher concentration of aldehydes, ketones, alkanes, carboxylic acids and lactones was observed, which are associated with the presence of the PE layer in the sample. These chemical groups together with alcohols, alkenes, fatty acids and methyl esters are among the reported degradation products of PE [50, 51]. Additionally, PET degradation products were also detected in the sample with 1st series cyclic dimers PET and suspected oligomers being detected in higher concentrations, when analyzed by liquid extraction. The suspected oligomers could not be positively confirmed because they were not included in the mass spectra database, but the fragmentation pattern showed the characteristic m/z 75.9, 103.9, 341, 385 and 429.1. Additionally, several peaks of relative intensity were tentatively identified as monododecyl ethers with varying numbers of ethylene glycol groups. Mechanical stress, pressure and chemical attack, which can occur during production and further processing, could have induced the formation of the detected breakdown products [52, 53].

The processed flakes (sample F-Rc) showed 132 tentatively identified peaks. Although many of the initially present components remained in the processed samples, in comparison

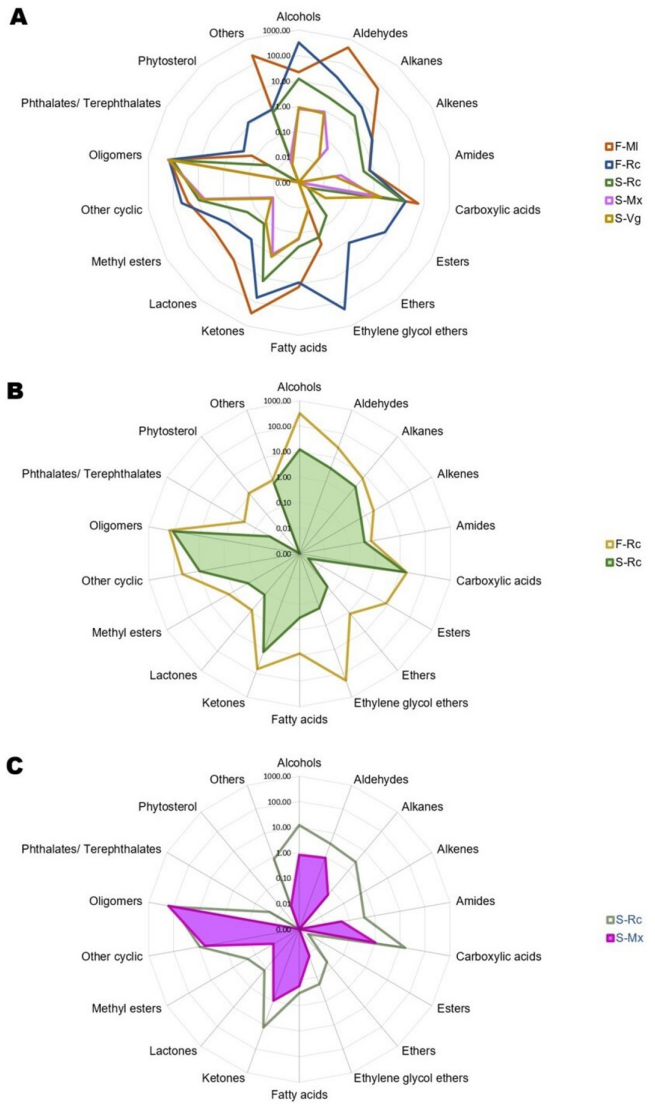

FIGURE 3 | (A) Semiquantification of the compounds detected. Comparison of the effect of (B) extrusion process and (C) mixing of rPET with vPET in the production of PET sheets.

to sample F-Ml, the overall concentration of aldehydes, lactones, alkanes and ketones had a reduction of 94%, 91%, 89% and 78%, respectively, in the F-Rc sample. This could be attributed to the removal of the PE layer suggesting the effectivity of the delamination process. A higher concentration of PET degradation products such as 1,3-dioxolane, which is a commonly reported NIAS in PET derived from ethylene glycol monomer, was observed [54–56]. Formic acid, which is formed due to thermal and hydrolytic degradation of PET was also detected. However, uncharacteristic large peaks of alcohols (cycloalcohol, 10-C and 12-C alcohols), various ethylene glycol ether compounds and decyl trifluoroacetate were detected indicating high amounts of these substances. Alcohols are one of the substances reported to be present in PET [57] while a compound from the same family as decyl trifluoroacetate was reported to be present in mechanically rPET [58]. Ethylene glycol ethers were previously detected in other rPET samples and are related to surfactants used in the washing of rPET. These compounds (1,3-dioxolane, decyl trifluoroacetate and heptaethylene glycol monododecyl ether) belong to Cramer Class III of toxicity, and therefore, their migration is of special interest for the safety of rPET.

Figure 3B shows how the concentration decreases when the sheet is formed (the sheet sample S-Rc shows 96 tentatively identified peaks). This indicates the effect of extrusion and sheet forming in the decrease in concentration of the volatile and semivolatile compounds. Common breakdown products of PET such as dimers, suspected oligomers and 1,3-dioxolane were still present in higher concentrations. Alcohols, ketones, aldehydes, acetic acid and 1,3-dioxolane were detected in the sample in relatively lower concentrations as compared to the rPET flakes sample. Benzaldehyde was also detected in the sample, which is associated as a degradation product of PET [54–56]. Significant decrease in the concentration of ethylene glycol ethers was also observed. Despite the lower concentration of these compounds in the sheet, the estimated migration is still relatively high: the migration of 1,3-dioxolane and the alkyl derivative is respectively 0.14 and 0.04 $mg\,kg^{-1}$, exceeding the threshold of toxicological concern of 90 $\mu g\,day^{-1}$ $person^{-1}$. Although it must be recognized that there is a high degree of overestimation in the estimates, the experimental validation of these migration values is recommended for safety assessment.

When mixed with vPET, only 56 peaks were tentatively identified (sample S-Mx). However, there is no significant difference when compared with the sample S-Vg (55 tentatively identified peaks). Both have high concentrations of other cyclic compounds, which are mostly PET degradation products—1,3-dioxolane 2-methyl, benzaldehyde and furfural. Aldehydes, alcohols, carboxylic acids and ketones were still present in both samples (Figure 3C).

3.6.2 | PET 1st Series Dimer and Trimer Quantification by LC–MS

The abundance of PET dimers and probable oligomers in all samples from the GC–MS analyses prompted the need for a confirmation and more precise quantification through LC–MS analysis. Two (2) PET oligomers were used as references. The first series PET cyclic dimer ($[TPA\text{-}EG]_2$) was used because it was the dimer tentatively identified in the GC–MS (liquid extraction). The first series PET cyclic trimer ($[TPA\text{-}EG]_3$) was chosen because it is one of the most frequent and abundant in rPET [59, 60]. Figure S3 (Supplementary information) presents the LC–MS chromatogram. Formation of oligomers in PET is an inevitable process; hence, it is one of the most common NIAS in PET packaging whether made from virgin or recycled material [61, 62]. Because total dissolution of the samples was necessary to extract the target compounds, sample F-Ml was not tested.

In general, all samples yielded higher concentrations of 1st series cyclic trimers than cyclic dimers (Figure 4). The highest concentration for both cyclic dimers and trimers was detected in sample S-Rc, 209 and 2885 $\mu g\,g^{-1}$, respectively. The concentration of trimer was significantly higher than for the flakes sample F-Rc (2083 $\mu g\,g^{-1}$), suggesting that the process of sheet production increased the concentration of these heavier oligomers. The value for the dimer is similar for the two samples and possibly the formation during sheet production may be compensated by

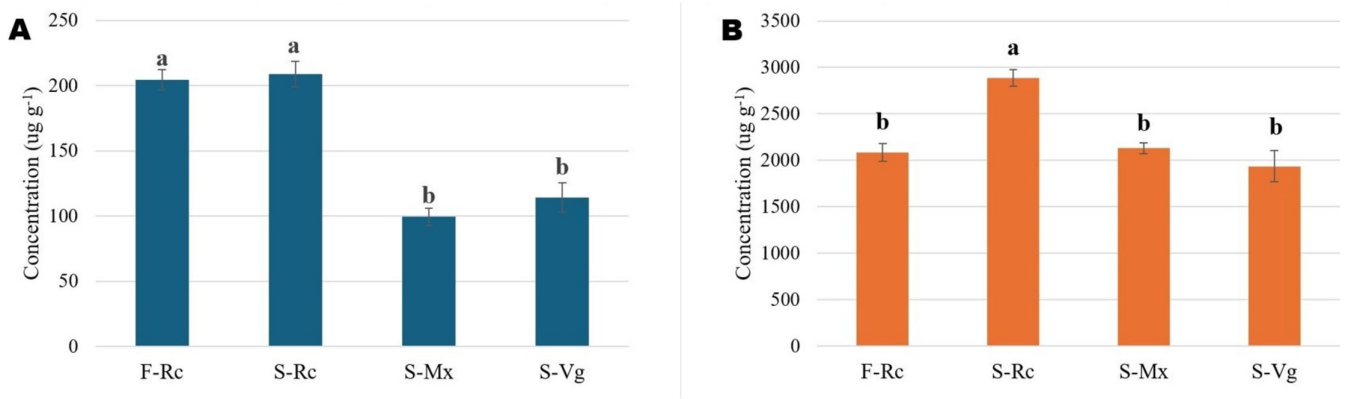

FIGURE 4 | Concentration of PET cyclic (A) 1st series cyclic dimers and (B) trimers *Data points associated with the same letter are statistically equivalent ($\alpha = 0.05$).*

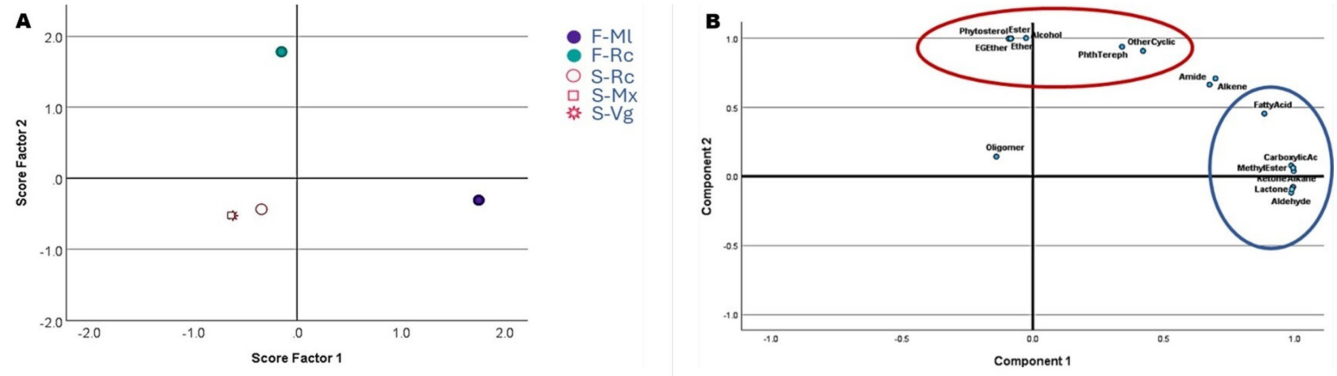

FIGURE 5 | PCA of potential migrants screening by GC–MS (A) Scatter plot (B) Plot of the contributors to each component.

the losses in the case of the lighter oligomers. The concentration of both cyclic dimers and trimers is significantly lower for the sample S-Vg (114 and 1936 $\mu g\,g^{-1}$). These results are comparable to studies conducted in rPET bottle and tray wherein higher concentrations of PET oligomers were observed in packages made from rPET [60, 63, 64]. rPET packaging tends to have more oligomers due to additional heat exposure occurring during the mechanical recycling process and extrusion, which promotes depolymerization [60]. The concentration of PET dimers and trimers in sample S-Mx (99 and 2129 $\mu g\,g^{-1}$) is not significantly different from sample S-Vg.

3.6.3 | Impact of Extrusion and Mixing With vPET

There was a significant decrease in the concentration of compounds detected after the extrusion of rPET flakes into rPET sheets. Most notably, ethylene glycol ethers, which were present in high concentration in rPET flakes decreased in the rPET sheets. All other compounds including alcohols, aldehydes, alkanes, amides, esters, ethers, fatty acids, ketones, lactones, methyl esters and other cyclic compounds had reduced concentrations, with the exception of carboxylic acids (formic acid) and oligomers (Figure 3B). Phytosterols were no longer detected in the rPET sheets. The high temperatures during the extrusion process reaching a maximum of 280°C possibly caused the degradation of some compounds and the release of volatile compounds.

As expected, mixing vPET with the rPET flakes further lowered the concentration of substances detected when producing the sheets (Sample S-Mx) due to the dilution effect (Figure 3C). A significant decrease in the concentration of almost all substances was observed. No ethers and alkenes were detected in the sample S-Mx. With this ratio of mixture, the resulting PET sheet shows a similar profile with sample S-Vg.

The results of the untargeted screening after semiquantification of the compounds detected were subjected to PCA. In Figure 5A, the scatter plot shows that the sheet samples were distinctly differentiated from the flakes sample. Sample F-Ml was discriminated from the rest of the samples by Factor 1 showing the contribution of PE. PCA results in Figure 5B indicate that the substances relevant to differentiate the initial flakes from the other samples are alkanes, aldehydes and ketones as main contributors to Factor 1. These substances are all degradation products of PE and were present in high amounts in the PET/PE flakes. The sample F-Rc was discriminated against the sheet samples by Factor 2. Figure 5B shows that substances from the delamination process such as alcohol, ethylene glycol ether, ester, ether and other cyclic compounds were the main contributors to component 2.

Sheet samples are easily discriminated from flakes. The distribution in the PCA (Figure 5B) plot is in agreement with the results of the GC–MS analysis with sample S-Rc appearing separated possibly due to the higher concentration of oligomers in

this sample and its contribution to Factor 2. This is also consistent with the PCA results of the IR spectroscopy of the samples.

4 | Conclusions

The delamination process resulted in the removal of more than 95% of PE from the multilayer flakes, enabling the resulting rPET flakes to be used in the production of new PET sheets. The physical and chemical properties of the rPET sheets were significantly influenced by the rPET content.

In terms of optical properties, no visible differences were observed between the rPET sheets and vPET sheets. However, spectrophotometric analysis revealed that the rPET content affected both the colour and haze of the sheets.

The thermal properties of the sheets were generally not greatly affected by rPET content, with the exception of cold crystallization. Sheets made from 100% rPET crystallized at a lower temperature than the other samples. A lower IV was also observed in the rPET sheets.

FTIR analysis combined with PCA highlighted differences between the spectra of recycled and virgin sheets. Residual tie-layer adhesive was detected in the recycled sheet. This combination of spectroscopy and data treatment proved useful for inferring the recycled content in mixed materials. Expanding this analysis to include more levels of rPET incorporation could yield further insights.

Chromatographic analysis revealed the presence of various potentially migratable substances, especially oligomers. Additional heat exposure during delamination and extrusion led to an increase in trimer content. However, the concentrations of many substances decreased after sheet formation. Notably, some PET degradation products classified as Cramer Class III (indicating high toxicity concern) were detected. Estimated migration levels, assuming total transfer, suggest that further studies are needed to assess the migration potential of these compounds. However, it should be recognized that assuming total mass transfer for such a low diffusivity polymer like PET largely overestimates the migration level.

This study, which characterizes substances detected in postindustrial samples, serves as a benchmark for future investigations on postconsumer trays, where additional contaminants from prior use, collection and sorting processes are expected.

Industrial guidelines on packaging design are crucial for addressing the recyclability and circularity challenges of multilayer PET trays. The delamination process, when aligned with current industry practices for washing and separating PET flakes, enables effective recovery of rPET. However, further investigation is needed to determine whether this process is equally effective when other types of adhesives are used.

Acknowledgements

The authors thank Evertis Iberia S.A. for the samples supply. Open access publication funding provided by FCT (b-on).

Data Availability Statement

The data that supports the findings of this study are available in the supplementary material of this article.

References

1. S. Engelmann, *Advanced Thermoforming: Methods, Machines and Materials, Applications, Automation, Sustainability, and the Circular Economy*, 2nd ed., (John Wiley & Sons, Inc., 2023), https://doi.org/10.1002/9781119666189.

2. R. Nisticò, "Polyethylene Terephthalate (PET) in the Packaging Industry," *Polymer Testing* 90 (2020): 106707, https://doi.org/10.1016/j.polymertesting.2020.106707.

3. ICIS 2024. PET Market in Europe State of Play: Production, Collection & Recycling Data 2022. https://www.plasticsrecyclers.eu/wp-content/uploads/2024/05/PET-Market-in-Europe-State-of-Play-2022-Data-V3.pdf.

4. C. Lee, Y.-C. Jang, K. Choi, B. Kim, H. Song, and Y. Kwon, "Recycling, Material Flow, and Recycled Content Demands of Polyethylene Terephthalate (PET) Bottles Towards a Circular Economy in Korea," *Environments* 11, no. 2 (2024): 25, https://doi.org/10.3390/environments11020025.

5. T. Muringayil Joseph, S. Azat, Z. Ahmadi, et al., "Polyethylene Terephthalate (PET) RECYCLING: A REVIEW," *Case Studies in Chemical and Environmental Engineering* 9 (2024): 100673, https://doi.org/10.1016/j.cscee.2024.100673.

6. M. K. Eriksen, J. D. Christiansen, A. E. Daugaard, and T. F. Astrup, "Closing the Loop for PET, PE and PP Waste From Households: Influence of Material Properties and Product Design for Plastic Recycling," *Waste Management* 96 (2019): 75–85, https://doi.org/10.1016/j.wasman.2019.07.005.

7. P. Benyathiar, P. Kumar, G. Carpenter, J. Brace, and D. K. Mishra, "Polyethylene Terephthalate (PET) Bottle-to-Bottle Recycling for the Beverage Industry: A Review," *Polymers* 14, no. 12 (2022): 2366, https://doi.org/10.3390/polym14122366.

8. J. Rossi and A. Bianchini, ""Plastic Waste Free" – A New Circular Model for the Management of Plastic Packaging in Food Value Chain," *Transportation Research Procedia* 67 (2022): 153–162, https://doi.org/10.1016/j.trpro.2022.12.046.

9. A. Barredo, A. Asueta, I. Amundarain, et al., "Chemical Recycling of Monolayer PET Tray Waste by Alkaline Hydrolysis," *Journal of Environmental Chemical Engineering* 11, no. 3 (2023): 109823, https://doi.org/10.1016/j.jece.2023.109823.

10. V. B. Gupta and Z. Bashir, "PET Fibers, Films, and Bottles: Sections 1–4.13," in *Handbook of Thermoplastic Polyesters*, ed. S. Fakirov (Wiley-VCH Verlag GmbH & Co. KGaA, 2002), 317–361, https://doi.org/10.1002/3527601961.ch7a.

11. V. H. Gabriel, A. Schaffernak, M. Pfitzner, J. Fellner, M. Tacker, and S. Apprich, "Rigid Polyethylene Terephthalate Packaging Waste: An Investigation of Waste Composition and Its Recycling Potential in Austria," *Resources* 12, no. 11 (2023): 128, https://doi.org/10.3390/resources12110128.

12. M. Seier, V.-M. Archodoulaki, T. Koch, B. Duscher, and M. Gahleitner, "Polyethylene Terephthalate Based Multilayer Food Packaging: Deterioration Effects During Mechanical Recycling," *Food Packaging and Shelf Life* 33 (2022): 100890, https://doi.org/10.1016/j.fpsl.2022.100890.

13. Petcore Europe. 2024. Design Guidelines - Transparent Clear PET Trays, https://www.tcep-europe.org/design-guidelines/products.

14. RecyClass. 2024. Design for Recycling Guidelines, https://recyclass.eu/recyclability/design-for-recycling-guidelines/.

15. G. Santomasi, R. Aquilino, M. Brouwer, et al., "Strategies to Enhance the Circularity of Non-Bottle PET Packaging Waste Based on a

Detailed Material Characterisation," *Waste Management* 186 (2024): 293–306, https://doi.org/10.1016/j.wasman.2024.06.016.

16. B. B. Turriziani, R. P. Vieira, L. Marangoni Júnior, and R. M. V. Alves, "Mechanical Recycling of Multilayer Flexible Packaging Employing Maleic Anhydride as Compatibilizer," *Journal of Polymers and the Environment* 32, no. 3 (2024): 1393–1405, https://doi.org/10.1007/s10924-023-03057-9.

17. M. Seier, V.-M. Archodoulaki, and T. Koch, "The Morphology and Properties of Recycled Plastics Made From Multi-Layered Packages and the Consequences for the Circular Economy," *Resources, Conservation and Recycling* 202 (2024): 107388, https://doi.org/10.1016/j.resconrec.2023.107388.

18. O. Horodytska, F. J. Valdés, and A. Fullana, "Plastic Flexible Films Waste Management – A State of Art Review," *Waste Management* 77 (2018): 413–425, https://doi.org/10.1016/j.wasman.2018.04.023.

19. C. T. de Mello Soares, M. Ek, E. Östmark, M. Gällstedt, and S. Karlsson, "Recycling of Multi-Material Multilayer Plastic Packaging: Current Trends and Future Scenarios," *Resources, Conservation and Recycling* 176 (2022): 105905, https://doi.org/10.1016/j.resconrec.2021.105905.

20. M. Babaei, M. Jalilian, and K. Shahbaz, "Chemical Recycling of Polyethylene Terephthalate: A Mini-Review," *Journal of Environmental Chemical Engineering* 12, no. 3 (2024): 112507, https://doi.org/10.1016/j.jece.2024.112507.

21. A. Schade, M. Melzer, S. Zimmermann, T. Schwarz, K. Stoewe, and H. Kuhn, "Plastic Waste Recycling—A Chemical Recycling Perspective," *ACS Sustainable Chemistry & Engineering* 12, no. 33 (2024): 12270–12288, https://doi.org/10.1021/acssuschemeng.4c02551.

22. British Plastics Federation. 2024. Thermoforming, https://www.bpf.co.uk/plastipedia/processes/Thermoforming.aspx#ReCycling.

23. T. Li, G. Theodosopoulos, C. Lovell, A. Loukodimou, K. K. Maniam, and S. Paul, "Progress in Solvent-Based Recycling of Polymers from Multilayer Packaging," *Polymers* 16, no. 12 (2024): 1670, https://doi.org/10.3390/polym16121670.

24. Ecosense Foundation 2022. Design for Recycling Guidelines for Thermoformed PET Packaging. https://ecosensefoundation.org/wp-content/uploads/2024/02/ecosense_foundation_recyclability_guidelines_jan22-5.pdf.

25. T. De Somer, M. Roosen, L. Harinck, K. M. Van Geem, and S. De Meester, "Removal of Volatile Components From Plastic Waste in Liquid Media: Effect of Temperature and Particle Size," *Resources, Conservation and Recycling* 182 (2022): 106267, https://doi.org/10.1016/j.resconrec.2022.106267.

26. S. D. Mancini, J. A. S. Schwartzman, A. R. Nogueira, D. A. Kagohara, and M. Zanin, "Additional Steps in Mechanical Recyling of PET," *Journal of Cleaner Production* 18, no. 1 (2010): 92–100, https://doi.org/10.1016/j.jclepro.2009.09.004.

27. F. W. Billmeyer, Jr., "Methods for Estimating Intrinsic Viscosity," *Journal of Polymer Science* 4, no. 1 (1949): 83–86, https://doi.org/10.1002/pol.1949.120040107.

28. T. Negoro, W. Thodsaratpreeyakul, Y. Takada, S. Thumsorn, H. Inoya, and H. Hamada, "Role of Crystallinity on Moisture Absorption and Mechanical Performance of Recycled PET Compounds," *Energy Procedia* 89 (2016): 323–327, https://doi.org/10.1016/j.egypro.2016.05.042.

29. I. T. Jolliffe, *Principal Component Analysis* (Springer-Verlag, 1986), https://books.google.pt/books?id=Km4ZAQAAIAAJ.

30. T. Næs, T. Isaksson, T. Fearn, and T. Davies, "A User-Friendly Guide to Multivariate Calibration and Classification," *Chemometrics and Intelligent Laboratory Systems* 71 (2004): 79–81, https://doi.org/10.1016/j.chemolab.2003.12.010.

31. A. Savitzky and M. J. E. Golay, "Smoothing and Differentiation of Data by Simplified Least Squares Procedures," *Analytical Chemistry* 36, no. 8 (1964): 1627–1639, https://doi.org/10.1021/ac60214a047.

32. EC (European Commission), "Commission Regulation No 10/2011 of 14 January 2011 on Plastic Materials and Articles Intended to Come into Contact with Food," *Official Journal of the European Communities No L* 12, no. 15/01/2011 (2011): 1–89.

33. Petcore Europe 2023a. Guidelines for Non-Intentionally Added Substances (NIAS) Evaluation in PET & rPET Materials and Thermoforms.

34. G. M. Cramer, R. A. Ford, and R. L. Hall, "Estimation of Toxic Hazard—A Decision Tree Approach," *Food and Cosmetics Toxicology* 16, no. 3 (1976): 255–276, https://doi.org/10.1016/S0015-6264(76)80522-6.

35. F. A. Chacon, M. T. Brouwer, and E. U. van Thoden Velzen, "Effect of Recycled Content and rPET Quality on the Properties of PET Bottles, Part I: Optical and Mechanical Properties," *Packaging Technology and Science* 33 (2020): 347–357, https://doi.org/10.1002/pts.2490.

36. Petcore Europe. 2023b. TCEP-P-08.- Sheet Extrusion, https://www.tcep-europe.org/download/18/tcep-p-08-sheet-extrusion.

37. O. Brandau, "2 - Material Basics," in *Stretch Blow Molding*, 2nd ed., ed. O. Brandau (William Andrew Publishing, 2012), 5–25, https://doi.org/10.1016/B978-1-4377-3527-7.00002-X.

38. T. B. Thomsen, K. Almdal, and A. S. Meyer, "Significance of Poly (Ethylene Terephthalate) (PET) Substrate Crystallinity on Enzymatic Degradation," *New Biotechnology* 78 (2023): 162–172, https://doi.org/10.1016/j.nbt.2023.11.001.

39. Y. Maruhashi and S. Iida, "Transparency of Polymer Blends," *Polymer Engineering and Science* 41, no. 11 (2001): 1987–1995, https://doi.org/10.1002/pen.10895.

40. L. Sangroniz, M. Fernández, and A. Santamaria, "Polymers and Rheology: A Tale of Give and Take," *Polymer* 271 (2023): 125811, https://doi.org/10.1016/j.polymer.2023.125811.

41. D. H. Kang, R. Auras, K. Vorst, and J. Singh, "An Exploratory Model for Predicting Post-Consumer Recycled PET Content in PET Sheets," *Polymer Testing* 30, no. 1 (2011): 60–68, https://doi.org/10.1016/j.polymertesting.2010.10.010.

42. S. Venkatachalam, G. N. Shilpa, V. L. Jayprakash, R. G. Prashant, R. Krishna, and K. K. Anil, "Degradation and Recyclability of Poly (Ethylene Terephthalate)," in *Polyester* (pp. Ch. 4, ed. M. S. H. El-Din (IntechOpen, 2012), https://doi.org/10.5772/48612.

43. Y. Celik, M. Shamsuyeva, and H. J. Endres, "Thermal and Mechanical Properties of the Recycled and Virgin PET—Part I," *Polymers* 14, no. 7 (2022): 1326, https://doi.org/10.3390/polym14071326.

44. L. Šudomová, H. Doležalová Weissmannová, Z. Steinmetz, V. Řezáčová, and J. Kučerík, "A Differential Scanning Calorimetry (DSC) Approach for Assessing the Quality of Polyethylene Terephthalate (PET) Waste for Physical Recycling: A Proof-of-Concept Study," *Journal of Thermal Analysis and Calorimetry* 148, no. 20 (2023): 10843–10855, https://doi.org/10.1007/s10973-023-12430-8.

45. A. Zarbali, I. Djaffar, and A. Menyhárd, "Prediction of Tensile Modulus Based on Parameters of Crystalline Structure in Polyethylene Terephthalate With Cold Crystallization Ability," *Heliyon* 10, no. 4 (2024): e26122, https://doi.org/10.1016/j.heliyon.2024.e26122.

46. L. Viora, M. Combeau, M. F. Pucci, et al., "A Comparative Study on Crystallisation for Virgin and Recycled Polyethylene Terephthalate (PET): Multiscale Effects on Physico-Mechanical Properties," *Polymers* 15, no. 23 (2023): 4613, https://doi.org/10.3390/polym15234613.

47. M. A. Peltzer and C. Simoneau, *ILC002 2013 - Identification of Polymeric Materials* (P. O. o. t. E. Union, 2013).

48. M. Bradley, *FTIR Basic Organic Functional Group Reference Chart* (ThermoFisher Scientific, 2015), https://www.thermofisher.com/blog/materials/a-gift-for-you-an-ftir-basic-organic-functional-group-reference-chart/.

49. M. Mecozzi and L. Nisini, "The Differentiation of Biodegradable and Non-Biodegradable Polyethylene Terephthalate (PET) Samples by FTIR

Spectroscopy: A Potential Support for the Structural Differentiation of PET in Environmental Analysis," *Infrared Physics & Technology* 101 (2019): 119–126, https://doi.org/10.1016/j.infrared.2019.06.008.

50. M. Hakkarainen and A.-C. Albertsson, "Environmental Degradation of Polyethylene," in *Long Term Properties of Polyolefins*, ed. A.-C. Albertsson (Springer, 2004), 177–200, https://doi.org/10.1007/b13523.

51. O. Horodytska, A. Cabanes, and A. Fullana, "Non-Intentionally Added Substances (NIAS) in Recycled Plastics," *Chemosphere* 251 (2020): 126373, https://doi.org/10.1016/j.chemosphere.2020.126373.

52. Y. Wang, G. Feng, N. Lin, et al., "A Review of Degradation and Life Prediction of Polyethylene," *Applied Sciences* 13, no. 5 (2023): 3045, https://doi.org/10.3390/app13053045.

53. Z. Yao, H. J. Seong, and Y.-S. Jang, "Environmental Toxicity and Decomposition of Polyethylene," *Ecotoxicology and Environmental Safety* 242 (2022): 113933, https://doi.org/10.1016/j.ecoenv.2022.113933.

54. A. Ozaki, E. Kishi, T. Ooshima, et al., "Determination of Potential Volatile Compounds in Polyethylene Terephthalate (PET) Bottles and Their Short- and Long-Term Migration Into Food Simulants and Soft Drink," *Food Chemistry* 397 (2022): 133758, https://doi.org/10.1016/j.foodchem.2022.133758.

55. E. U. Thoden van Velzen, M. T. Brouwer, C. Stärker, and F. Welle, "Effect of Recycled Content and rPET Quality on the Properties of PET Bottles, Part II: Migration," *Packaging Technology and Science* 33, no. 9 (2020): 359–371, https://doi.org/10.1002/pts.2528.

56. A. K. Undas, M. Groenen, R. J. B. Peters, and S. P. J. van Leeuwen, "Safety of Recycled Plastics and Textiles: Review on the Detection, Identification and Safety Assessment of Contaminants," *Chemosphere* 312 (2023): 137175, https://doi.org/10.1016/j.chemosphere.2022.137175.

57. A. Cabanes, F. J. Valdés, and A. Fullana, "A Review on VOCs From Recycled Plastics," *Sustainable Materials and Technologies* 25 (2020): e00179, https://doi.org/10.1016/j.susmat.2020.e00179.

58. S. Wu, X. Wu, H. Li, et al., "The Characterization and Influence Factors of Semi-Volatile Compounds From Mechanically Recycled Polyethylene Terephthalate (rPET) by Combining GC×GC-TOFMS and Chemometrics," *Journal of Hazardous Materials* 439 (2022): 129583, https://doi.org/10.1016/j.jhazmat.2022.129583.

59. S. Ubeda, M. Aznar, and C. Nerín, "Determination of Oligomers in Virgin and Recycled Polyethylene Terephthalate (PET) Samples by UPLC-MS-QTOF," *Analytical and Bioanalytical Chemistry* 410, no. 9 (2018): 2377–2384, https://doi.org/10.1007/s00216-018-0902-4.

60. G. Colombo, M. Corredig, I. Uysal Ünalan, and E. Tsochatzis, "Untargeted Screening of NIAS and Cyclic Oligomers Migrating From Virgin and Recycled Polyethylene Terephthalate (PET) Food Trays," *Food Packaging and Shelf Life* 41 (2024): 101227, https://doi.org/10.1016/j.fpsl.2023.101227.

61. M. Hoppe, P. de Voogt, and R. Franz, "Identification and Quantification of Oligomers as Potential Migrants in Plastics Food Contact Materials With a Focus in Polycondensates – A Review," *Trends in Food Science & Technology* 50 (2016): 118–130, https://doi.org/10.1016/j.tifs.2016.01.018.

62. V. N. Schreier, C. Appenzeller-Herzog, B. J. Brüschweiler, et al., "Evaluating the Food Safety and Risk Assessment Evidence-Base of Polyethylene Terephthalate Oligomers: Protocol for a Systematic Evidence Map," *Environment International* 167 (2022): 107387, https://doi.org/10.1016/j.envint.2022.107387.

63. D. Diamantidou, E. Tsochatzis, S. Kalogiannis, J. Alberto Lopes, G. Theodoridis, and H. Gika, "Analysis of Migrant Cyclic PET Oligomers in Olive Oil and Food Simulants Using UHPLC-qTOF-MS," *Food* 12, no. 14 (2023): 2739, https://doi.org/10.3390/foods12142739.

64. M. Hoppe, R. Fornari, P. de Voogt, and R. Franz, "Migration of Oligomers From PET: Determination of Diffusion Coefficients and Comparison of Experimental Versus Modelled Migration," *Food Additives & Contaminants: Part A* 34, no. 7 (2017): 1251–1260, https://doi.org/10.1080/19440049.2017.1322222.

Supporting Information

Additional supporting information can be found online in the Supporting Information section. **Table S1:** Mixture of standards used for the semiquantification of the gas chromatography–mass spectrometry (GC–MS) results. **Figure S1:** GC–MS chromatogram of headspace analysis for PET/PE flakes (up) and 100% rPET flakes (down). Tentatively identified peaks: *1—formic acid; 2—cyclohexanol 2-methyl-; 3–1-heptanol, 2-propyl-; 4–2-dodecanol; 5- diethylene glycol monododecyl ether.* **Figure S2:** GC–MS chromatogram of liquid extraction analysis for PET/PE flakes (up) and 100% rPET flakes (down). Tentatively identified peaks: *1—1st series PET cyclic dimer; 2, 3 and 4—tentatively identified as PET oligomers through m/z fragmentation pattern; *—tentatively identified as n (ethylene glycol) monododecyl ethers.* **Table S2:** LC–QQQ–MS source and acquisition parameters used for the determination of PET cyclic dimer and trimer. **Table S3:** LC–QQQ–MS calibration and performance for PET cyclic dimer and trimer. **Figure S3:** LC–MS chromatogram of target analysis for dimer and trimer 1st series cyclic PET oligomers. **Table S4:** List of 20 most abundant substances tentatively identified by GC–MS in PET samples. **Table S5:** Summary of the differential scanning calorimetry (DSC) results. **Figure S4:** DSC thermograms of samples (**above**) S-Vg and (**below**) S-Rc.